ELSEVIER

Journal of Non-Crystalline Solids 307–310 (2002) 679–687

JOURNAL OF NON-CRYSTALLINE SOLIDS

www.elsevier.com/locate/jnoncrysol

Segmental and normal mode dynamics during network formation

Jovan Mijovic *, Jo-Wing Sy

Department of Chemical Engineering and Chemistry, The Herman F. Mark Polymer Research Institute, Polytechnic University, Six Metrotech Center, Brooklyn, NY 11201, USA

Abstract

Broad-band dielectric relaxation spectroscopy was used to investigate the molecular dynamics of reactive systems where one of the components exhibits, in addition to the transverse dipole moment component ($\mu_\perp$ or type B) that gives rise to the segmental α process, a persistent cumulative dipole moment along the chain contour ($\mu_\parallel$ or type A). The systems studied were composed of an amine-terminated poly(propylene oxide) (PPO), that contains type A and B dipoles, and a bifunctional epoxy prepolymer. The segmental and normal mode processes were clearly discernible in the neat PPO and the PPO/epoxy blends with PPO MW $>$ 2000 g/mol. The α process broadens upon mixing. The normal mode has a narrower spectrum than the segmental mode and is not affected by mixing. Cross-linking causes the segmental and normal modes to gradually overlap and we observe a deviation of the normal mode from the Rouse dynamics and a considerable broadening of the α process. The molecular architecture of the growing network plays an important role in determining the dynamics, as the compositional and spatial heterogeneities arise during cross-linking. Interestingly, while the increased heterogeneity results in the broadening of the relaxation spectra, the temperature dependence of the α process remains unaffected by cross-linking. This is a curious finding; the apparent lack of a direct correlation between non-exponentiality and fragility in cross-linking PPO networks may reflect the length scale of relaxation and warrants further investigation.

PACS: 77.84.Jd; 71.45.Gm

1. Introduction

Complex polymeric structures whose dynamics have been studied thus far are predominately of the time-invariant nature [1] and only limited information is available on the dynamics of systems that undergo a temporal evolution of structure as a result of various chemical and physical transformations, such as chemical cross-linking, crystallization or phase separation [2]. In the past several years we have investigated the dynamics of a number of such time-variant systems that include reactive polymer networks [3], crystallizing polymers and blends [4], liquid crystalline polymers [5] and nano-structured amphiphilic block co-polymer/polymer network mixtures [6].

* Corresponding author. Tel.: +1-718 260 3097; fax: +1-718 260 3125.

E-mail address: jmijovic@poly.edu (J. Mijovic).

0022-3093/02/$ - see front matter
PII: S0022-3093(02)01532-6

The work described herein adds a new dimension to the studies of dipole dynamics in network-forming polymeric systems. Of interest here was to investigate the dynamics of reactive systems where one of the components exhibits, in addition to the transverse dipole moment component ($\mu_\perp$) that gives rise to the segmental α process, a persistent cumulative dipole moment along the chain contour ($\mu_\parallel$). This part of the dipole moment of the polymer molecule is present when the repeat unit lacks a plane of symmetry perpendicular to the chain contour and it can be relaxed via the normal mode process, termed α_N. The objective of this study is to provide an initial insight into the fundamental features *of* and the interplay *between* the segmental (α) and global (α_N) dynamics of polymer networks as they form.

2. Background

The pioneering research of Walter Stockmayer and co-workers in the 1960s led to the classification of dipole components in chain molecules into three types [7]: (1) type A – a dipole component is parallel to the chain contour; (2) type B – a dipole component is perpendicular to the chain contour; and (3) type C – a dipole component is located in the side group. The presence of two dielectric dispersions (types A and B) was first reported by Baur and Stockmayer in their study of poly(propylene oxide) or PPO [8].

It was not until the 1980s, however, that several groups resumed research on the dynamics of polymers with type A dipoles and subsequent developments took place. Most studies were conducted in dilute, semi-dilute and concentrated solutions of polymers that included poly(2,6-dichloro-1, 4-phenylene oxide) [9], polychloroprene [10], *cis*-polyisoprene (PI) [11–13], polyphenoxyphosphazine [14] and polylactones [15]. Bulk *cis*-PI was first studied by Adachi and Kotaka [16], and later by Boese and Kremer [17]. Beevers et al. [18] conducted dielectric measurements on entangled PPO and contrasted the experimental results with the prediction of the reptation theory. Ngai studied bulk poly(propylene glycol), PPG, and used his coupling model to successfully describe the dielectric relaxation [19]. Watanabe et al. [20] were first to study *cis*-PI with the dipole sequence inverted (reversed) along the chain contour. Nicolai and Floudas compared dielectric and viscoelastic response of PPO diols and triols [21].

The interest in more complex (than linear) polymer systems grew in recent years. Watanabe et al. studied *cis*-PI/polybutadiene (PB) blends and found that an increase in the molecular weight of PB increased the normal mode relaxation time [22]. The normal mode relaxation of *cis*-PI in blends with vinyl poly(butadienes) was investigated by Schroeder and Roland who suggested that reptation and constraint release are not independent processes [23]. Karatasos et al. studied poly(styrene-b-1,4-isoprene) diblock co-polymers and detected, in the ordered state, a new relaxation process related to the coherently ordered microstructure [24]. An investigation of segmental and chain dynamics of PI in block co-polymer/homopolymer blends revealed that the block co-polymer microdomains provide a controlled confinement that affects both local and global dynamics [25]. There are several excellent review articles that discuss the dynamics of non-reactive polymers with type A dipoles [26–28].

In a recent study, Nicolai et al. [29] reported that the dynamics of entangled and cross-linked PPO melts were identical (when the molecular weight for entanglements was equal to that between the cross-links). However, there are no reports in the literature on a systematic study of the dynamics during chemical cross-linking of PPO-epoxy networks.

3. Experimental

3.1. Materials

The system studied was composed of an epoxy prepolymer and an amine-terminated PPO – their chemical structures are shown in Fig. 1. The epoxy prepolymer was diglycidylether of bisphenol A (DGEBA, $n \approx 0$, MW = 374 g/mol). Three different molecular weights of PPO (Aldrich) were used; 400, 2000 and 4000 g/mol (code: PPO-400, PPO-2000 and PPO-4000, respectively). We note that

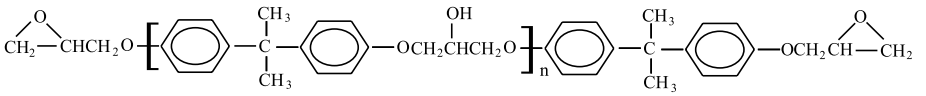

DGEBA

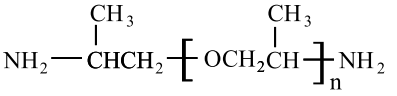

Amine Terminated PPO

Fig. 1. Chemical structure of the components used in this study.

the PPO chains contain two inverse sequences of type A dipoles and hence the normal mode process is dielectrically active even when the end junctions in the network are fixed. Measurements were made on three groups of samples: (1) individual components, (2) mixtures prior to the onset of reaction, and (3) mixtures during cross-linking. The epoxy prepolymer and the amine-terminated PPO (MW = 400, 2000 and 4000) were mixed in the stoichiometric ratio: these mixtures are referred in the text as EPPO-400, EPPO-2000 and EPPO-4000, respectively.

3.2. Techniques

Dielectric Relaxation Spectroscopy. Our facility combines commercial and custom-made instruments that include (1) Novocontrol's α high resolution dielectric analyzer (3 μHz–10 MHz), (2) Solartron 1260 impedance/gain phase analyzer (10 μHz–32 MHz), (3) Hewlett–Packard 4284A LCR meter (20 Hz–1 MHz), (4) Hewlett–Packard 8752A network analyzer (300 kHz–1.3 GHz) and (5) Hewlett-Packard 4291B RF impedance analyzer (1 MHz–1.8 GHz). All instruments are interfaced to PCs and equipped with heating/cooling capabilities, including a custom-modified Novocool system [30].

Supporting Techniques. Supporting evidence was obtained from Fourier transform infrared spectroscopy in near-IR and mid-IR range [31], and differential scanning calorimetry.

4. Results and discussion

4.1. Individual components and blends prior to onset of chemical reaction

We start our discussion by a brief examination of the DSC T_g, determined according to the protocol suggested by Angell [32]. The effect of molecular weight on the T_g of PPO was negligible, as seen in Table 1. The measured T_g was between 195.5 and 198 K. The T_g of DGEBA was 255 K, about 60 K higher than that of PPO. The T_gs of DGEBA/PPO blends increase with decreasing molecular weight of PPO (due to an increase of the DGEBA content). We shall examine the other entries in Table 1 later.

The dielectric response of DGEBA (not shown here) was examined first. The segmental α process is located at about 80 Hz at −5 °C and the spectrum is skewed to high frequency due to the presence of the β process. The normal mode relaxation is absent in PPO-400, but is evident in PPO-2000 and PPO-4000. Dielectric loss in the frequency domain (12 decades) with temperature as a parameter for PPO-4000 is shown in Fig. 2. Note how the temperature dependence of normal and segmental modes is beautifully discerned. The Havriliak–Negami (HN) [33], and the Kohlrausch–Williams–Watts (KWW) [34], functional forms provide good fits for normal and segmental processes in PPO-2000 and PPO-4000. A comparison of the shape parameters of the relaxation

Table 1
Characteristic relaxation parameters for individual components and as-mixed blends

Materials	T_g[a]	T_g^*[b]	T_0 (K)[c]	τ_0^s (s)[c]	B^s (K)[c]	τ_0^n (s)[c]	B^n (K)	$F_{1/2}$[d]
DGEBA	255.5	254.7	224.6	1×10^{-14}	1105	–	–	0.79
PP-400	195.6	196.2	159.5	1×10^{-14}	1351	–	–	0.69
PP-2000	198.1	196.3	160.5	1×10^{-14}	1317	7.6×10^{-12}	1191	0.69
PP-4000	198.7	196.8	159.9	1×10^{-14}	1361	1.1×10^{-10}	1209	0.68
EP-400	225.5	227.9	192.6	1×10^{-14}	1301	–	–	0.73
EP-2000	209.8	210.4	173.9	1×10^{-14}	1345	1.3×10^{-11}	1149	0.70
EP-4000	207.0	205.8	169.1	1×10^{-14}	1352	1.4×10^{-10}	1157	0.70

[a] obtained from DSC measurements, onset definition.
[b] T_g^*: defined as the temperature at $\tau = 100$ s.
[c] T_0, τ_0, B of the VFT equation: s – local segmental mode; n – normal mode.
[d] $F_{1/2}$ (see Ref. [34]).

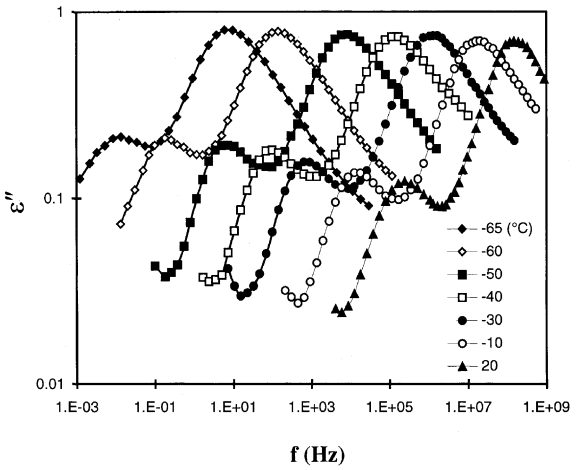

Fig. 2. Dielectric loss in the frequency domain with temperature as a parameter for PPO-4000.

Table 2
HN and KWW best fit parameters for individual components and as-mixed blends

	Local segmental mode (α)			Normal mode		
	a[a]	b[a]	β[b]	a[a]	b[a]	β[b]
DGEBA	0.88	0.45	0.5	–	–	–
PPO-400	0.53	0.7	–	–	–	–
PPO-2000	0.84	0.43	0.49	0.9	0.58	0.62
PPO-4000	0.83	0.44	0.49	0.89	0.59	0.62
EPPO-400	0.68	0.38	0.35	–	–	–
EPPO-2000	0.65	0.52	0.40	0.9	0.59	0.62
EPPO-4000	0.71	0.51	0.42	0.91	0.59	0.62

[a] a, b are the shape parameters of the HN equation.
[b] β parameter of the KWW equation.

spectra of different samples, about 30 °C above their respective T_gs, is provided in Table 2. Note that the α process of PPO-400 cannot be described by the KWW equation, because it has a more symmetric spectrum (large b in the HN function).

As seen in Table 1, the segmental α process in the as-mixed blends (EPPO-2000 and EPPO-4000) becomes broader (smaller HN a and KWW β) and more symmetric (greater HN b) upon mixing. The experimentally observed broadening of the glass transition in polymer blends has been attributed to the concentration fluctuations that give rise to a dynamically heterogeneous environment in a globally miscible blend [35]. Alternatively, an argument based on Ngai's coupling model invokes concentration fluctuations that effectively produce the distributed coupling parameter for each component, thereby resulting in the broadening of the T_g [36]. The effect of mixing is more pronounced in EPPO-2000 than in EPPO-4000, probably due to the higher concentration (and hence enhanced fluctuations) of DGEBA in the former blend. The effect of concentration fluctuations diminishes with increasing length scale of motion and that explains why the shape of the normal mode relaxation spectrum varies little between different samples. Note that the normal mode process is narrower than the α process.

We next examine the temperature dependence of the average relaxation time for segmental and normal mode, defined as $\tau = 1/\omega = 1/2\pi f_{max}$, where f_{max} is the frequency at maximum loss. The relaxation maps for segmental and normal processes in various samples are shown in Fig. 3(A)

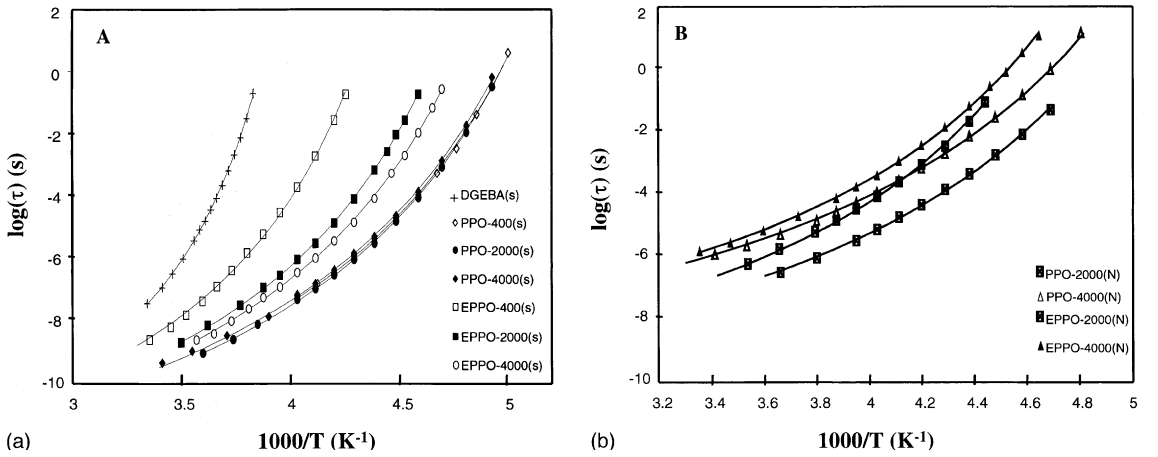

Fig. 3. Plots of the average relaxation time for segmental mode (A) and normal mode (B) as a function of reciprocal temperature for various systems. Plot C shows the T_g-scaled temperature dependence of the average relaxation time for the segmental process.

and (B), respectively. All relaxations bear a strong signature of the glass transition (curvature) and are well described by the Vogel–Fulcher–Tammann (VFT) equation (solid lines are VFT fits). The effect of molecular weight on the average relaxation time for the normal mode is readily noted. Excellent fits of the α process were obtained by fixing τ_0^s at the attempt frequency of 10^{-14} s (the superscript s denotes segmental mode). However, this constraint cannot be applied to the normal mode process, where τ_0^n is significantly greater than 10^{-14} s for good VFT fits. Interestingly, by making T_0 equal to the value obtained for the α process, we were able to generate excellent VFT fits for the normal mode relaxation. All fitting parameters are summarized in Table 1.

Of interest was to examine how the ratio of relaxation times for segmental and normal modes varies with temperature. We write $\tau_s(T)/\tau_n(T) = (\tau_0^s/\tau_0^n)\exp(B_s - B_n)/(T - T_0)$, where s and n denote segmental and normal mode, respectively, and τ_0, B and T_0 are the VFT fit parameters. Since $B_s > B_n$, the relaxation time for the α process will approach that for the normal mode with decreasing temperature. In PPO-4000, for example, τ_s is about four orders of magnitude greater than τ_n at 'infinite' temperature, while the α process becomes slower than the normal mode below 176 K, about 20 K below the glass transition. But the extrapolated crossover will not happen and an explanation is given by Ngai [37]. How decreasing temperature slows down different relaxation mechanisms can be also gleaned from a plot of the ratio of the relaxation times for segmental and normal modes versus the relaxation time for segmental mode (Fig. 4). Of interest is how the addition of DGEBA affects the evolution of encroachment across the T_g range. Both sets of curves (PPO-4000/EPPO-4000 and PPO-2000/EPPO-2000) merge at short

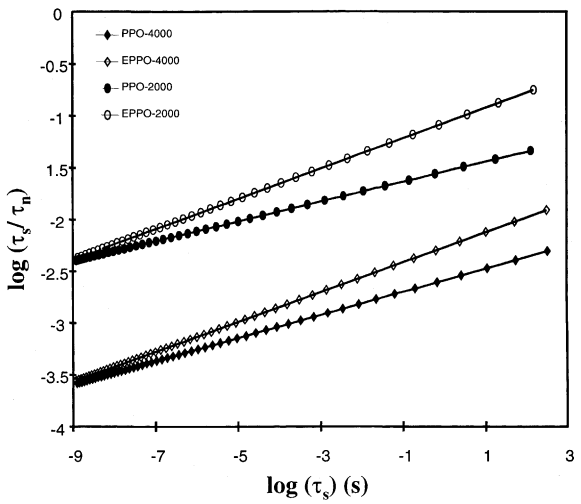

Fig. 4. Ratio of segmental and normal mode relaxation time versus segmental mode relaxation time for samples of different composition and molecular weight.

relaxation times and diverge as the relaxation time of the α process increases. Interestingly, the normal mode process is faster in EPPO than in PPO under the condition of equal segmental relaxation time. This trend increases with increasing relaxation time for the segmental mode and is slightly more pronounced in the lower molecular weight sample. This observation further suggests that the addition of DGEBA to PPO does not affect equally the dynamics of normal and segmental modes and we are currently exploring this issue further.

The temperature dependence of the average relaxation time for the α process was further analyzed using the concept of fragility [38]. The calculated fragility indices are summarized in Table 1. The fragility plots (not shown here) for neat PPO and for DGEBA/PPO blends are similar, with $F_{1/2}$ of about 0.64. This may be attributed to the relatively small weight content of DGEBA in the blends. Neat DGEBA is a more fragile glass former, with $F_{1/2}$ of about 0.79. But despite the observed difference in fragility, DGEBA and PPOs have identical KWW β of 0.5. This is very interesting because it suggests that the concentration fluctuations that contribute to the broadening of the α spectrum may not play a crucial role in determining the temperature dependence of the average relaxation time.

4.2. Dipole dynamics during network formation

In this section we examine the effect of cross-linking on the dielectric response. We start by describing the system that does not show normal mode relaxation, namely EPPO-400. In Fig. 5 we show dielectric loss with reaction time as a parameter for EPPO-400 at 25 °C. Data were generated during reaction according to the methodology suggested by Williams and co-workers [39]. The average relaxation time of the mixture prior to the onset of reaction is about one nanosecond. The observed shift of the loss peak to lower frequency during reaction reflects a decrease in the mobility and an increase in the network T_g. The splitting of α and β processes during reaction is evident. Since the reaction temperature of 25 °C is below the $T_{g\infty}$, the network vitrifies prior to the completion of

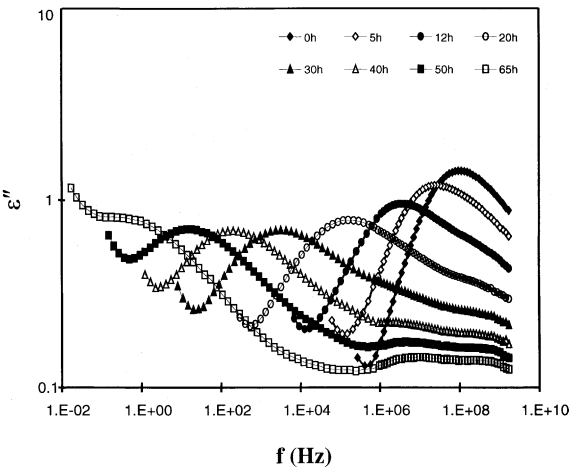

Fig. 5. Dielectric loss in the frequency domain with reaction time as a parameter during cross-linking of EPPO-400 at 25 °C.

cure. An alternative approach to following the effect of the progress of reaction on dynamics consists in conducting sweeps on the networks quenched at selected degrees of cross-linking. The requirement that the reaction is negligible during the sweep over the temperature range of interest is readily satisfied in this system. Moreover, since PPO also bears non-reactive dipoles (Class 2 network-formers, see Ref. [40]), the dielectric signal remains strong throughout the reaction.

The temperature dependence of the average relaxation time at various extents of cross-linking in EPPO-400 is shown in Fig. 6. All curves are well described by the VFT equation and the best-fit parameters are summarized in Table 3. A pronounced increase in T_g during cross-linking is evident. Interestingly, the fragility of the network does not vary during cross-linking (see Table 3), but the relaxation spectra are systematically broadened. Because the α process is thermodielectrically simple for an iso-structural network, the observed broadening is a direct consequence of the effect of cross-linking on network dynamics.

We now turn attention to EPPO-2000 and EPPO-4000 systems, where both segmental and normal modes are clearly identifiable prior to the onset of reaction. During cross-linking, the α process shifts to lower frequency, diminishes in intensity and broadens, as exemplified in Fig. 7 for

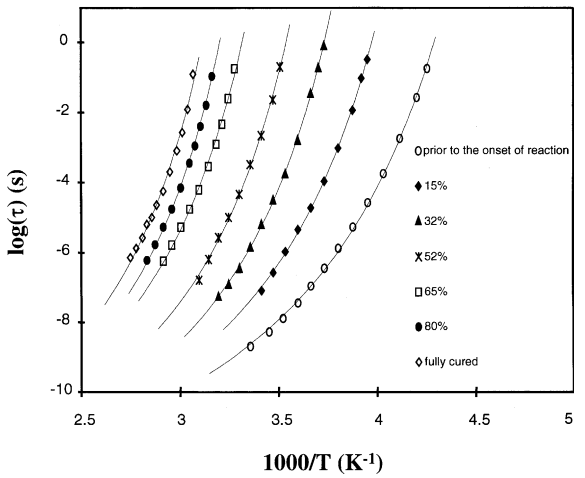

Fig. 6. Average relaxation time as a function of reciprocal temperature with extent of cross-linking as a parameter for EPPO-400.

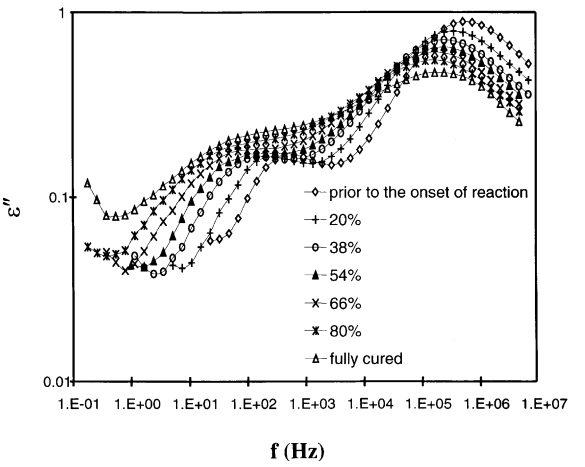

Fig. 7. Dielectric loss in the frequency domain with extent of cross-linking as a parameter for EPPO-4000 at −25 °C.

Table 3
VFT parameters and fragility as a function of degree of cross-linking for EPPO-400

Extent of reaction	T_g^* (K)[a]	T_0 (K)[b]	τ_0 (s)[b] $\times 10^{-14}$	B (K)[b]	$F_{1/2}$[c]
Prior to reaction	227.9	192.6	1.0	1301	0.73
15%	246.3	209.9	1.0	1341	0.74
32%	262.5	225.9	1.0	1351	0.75
52%	276.8	237.5	1.0	1451	0.75
65%	294.9	250.2	1.0	1649	0.74
80%	305.7	261.6	1.0	1623	0.75
Fully cured	314.1	268.2	1.0	1700	0.74

[a] T_g^* defined as the temperature at $\tau = 100$ s.
[b] T_0, τ_0, B of the VFT equation.
[c] $F_{1/2}$ (see Ref. [38b]).

the as-mixed EPPO-4000. The normal mode process shifts to lower frequency at low conversion and overlaps with the α process at high conversion. The DSC T_g increases by ≈2 °C at the end of cure. The change in the relaxation spectrum for EPPO-2000 (not shown) is more pronounced because of the closer proximity of normal and segmental modes in this lower MW sample. The α process broadens considerably and can be followed up to about 70% conversion; beyond that it overlaps with the normal mode process. The dielectric relaxation strength ($\Delta\varepsilon$) of both processes decreases with the advancement of cross-linking and an attempt to quantify the temporal evolution of ($\Delta\varepsilon$) is currently underway.

An important question is to what point the normal and segmental relaxations can be treated as separate processes in the course of network formation. We attempted to provide an answer by deconvoluting and analyzing the relaxation spectra at various stage of cross-linking. The starting point in the analysis was to extract the shape parameters for segmental and normal mode relaxations from the non-reacted mixture and to use those values as reference. For EP-4000, the shape parameters of the α process varied from the early stage of reaction (even below 10% conversion) and the imposition of constant shape resulted in poor deconvolution. Fixing the shape parameters of the normal mode process also results in poor deconvolution after ≈20% conversion, suggesting that the observed broadening during cross-linking cannot be attributed exclusively to the α process. More can be learned by considering the distribution of relaxation times with degree of cross-linking as a parameter. This is exemplified in Fig. 8 for EPPO-2000. A distinct bimodal distribution is obtained prior to the nset of reaction. Both peaks become broader during cross-linking and eventually we observe a plateau between the two distributions. The presence of a plateau in the distribution plot

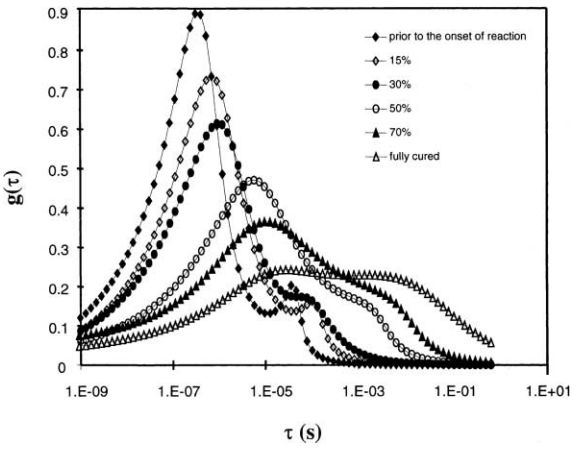

Fig. 8. Distribution of relaxation times with extent of cross-linking as a parameter for EPPO-2000 at −20 °C.

is evidence that the normal and segmental modes become coupled during cross-linking. At that point the Rouse model is no longer appropriate for describing chain dynamics. It is clear that the onset of encroachment in the time domain (changing network structure at a constant T) and the temperature domain (changing T at a constant network structure) depends on molecular architecture and co-operativity; the question is when exactly the encroachment sets in? Efforts along those lines are currently underway in our laboratory.

5. Conclusions

We have completed an initial investigation of the molecular dynamics of end-linked PPO networks at various degrees of cross-linking. The principal conclusions are as follows. The local segmental mode is a stronger function of temperature than the normal mode and encroachment sets in with decreasing temperature. The advancement of cross-linking leads to the coupling of segmental and normal modes, a deviation of the normal mode from the Rouse dynamics and a considerable broadening of the α process. The network architecture plays an important role in determining the dynamics: the compositional and spatial heterogeneities that arise during cross-linking depend on the molecular weight and chemical structure of the components. Increased heterogeneity results in the broadening of the relaxation spectra but the temperature dependence of the α process remains unaffected by cross-linking. This is an interesting observation; the apparent lack of a direct correlation between non-exponentiality and fragility in cross-linking PPO networks warrants further investigation.

Acknowledgements

This material is based on work supported by National Science Foundation under grant no. DMR-0101182.

References

[1] Extensive accounts of relaxation in glass formers can be found in the following special issues: (a) three volumes of J. Non-Cryst. Solids 131–133 (1991), 172–174 (1994); 235–237 (1998);
(b) K.L. Ngai et al. (Eds.), Glasses and Glass Formers: Current Issues, Mater. Res. Soc. Symp. Proc. Series, vol. 455, MRS, Pittsburgh, PA, 1997;
(c) Special issue of J. Res. NIST (1997) 102;
(d) Special issue of J. Phys. Chem. (1999) 103.
[2] G. Williams, in: E. Riande (Ed.), Keynote Lectures in Selected Topics of Polymer Science, CSIC, Madrid, 1997, p. 1, Chapter 1.
[3] B. Fitz, J. Mijovic, Macromolecules 32 (1999) 4134.
[4] J.-W. Sy, J. Mijovic, Macromolecules 33 (2000) 933.
[5] J. Mijovic, J.-W. Sy, Macromolecules 33 (2000) 9620.
[6] J. Mijovic, M. Shen, J.-W. Sy, I. Mondragon, Macromolecules 33 (2000) 5235.
[7] W.H. Stockmayer, Pure Appl. Chem. 15 (1967) 539.
[8] M.E. Baur, W.H. Stockmayer, J. Chem. Phys. 43 (1965) 4319.
[9] K. Adachi, T. Kotaka, Macromolecules 16 (1983) 1936.
[10] K. Adachi, T. Kotaka, Macromolecules 18 (1985) 295.
[11] (a) K. Adachi, T. Kotaka, Macromolecules 20 (1987) 2018;
(b) K. Adachi, T. Kotaka, Macromolecules 21 (1988) 157.
[12] S.S. Patel, K.M. Takahashi, Macromolecules 25 (1992) 4382.
[13] H. Watanabe, H. Yamada, O. Urakawa, Macromolecules 28 (1995) 6443.
[14] S. Uzaki, K. Adachi, T. Kotaka, Macromolecules 21 (1988) 153.
[15] (a) M.B. Baysal, W.H. Stockmayer, Macromolecules 27 (1994) 7429;
(b) O. Urakawa, K. Adachi, T. Kotaka, Y. Takemoto, H. Yasuda, Macromolecules 27 (1994) 7410.

[16] (a) K. Adachi, T. Kotaka, Macromolecules 17 (1984) 120; (b) K. Adachi, T. Kotaka, Macromolecules 18 (1985) 466.
[17] D. Boese, F. Kremer, Macromolecules 23 (1990) 829.
[18] M.S. Beevers, D.A. Elliott, G. Williams, Polymer 21 (1980) 13.
[19] K.L. Ngai, R.W. Rendell, Macromolecules 20 (1987) 1066.
[20] (a) H. Watanabe, O. Urakawa, T. Kotaka, Macromolecules 26 (1993) 5073;
(b) H. Watanabe, O. Urakawa, T. Kotaka, Macromolecules 27 (1994) 3525.
[21] T. Nicolai, G. Floudas, Macromolecules 31 (1998) 2578.
[22] H. Watanabe, O. Urakawa, H. Yamada, M.-L. Yao, Macromolecules 29 (1996) 755.
[23] M.J. Schroeder, C.M. Roland, Macromolecules 32 (1999) 2000.
[24] K. Karatasos, S.H. Anastasiadis, G. Floudas, G. Fytas, S. Pispas, N. Hadjichristidis, T. Pakula, Macromolecules 29 (1996) 1326.
[25] G. Floudas, K. Meramveliotaki, N. Hadjichristidis, Macromolecules 32 (1999) 7496.
[26] K. Adachi, T. Kotaka, Prog. Polym. Sci. 18 (1993) 585.
[27] K. Adachi, in: J.P. Runt, J.J. Fitzgerald (Eds.), Dielectric Spectroscopy of Polymeric Materials, American Chemical Society, Washington, DC, 1997, p. 261, Chapter 9.
[28] H. Watanabe, Prog. Polym. Sci. 24 (1999) 1253.
[29] T. Nicolai, F. Prochazka, D. Durand, Phys. Rev. Lett. 82 (1999) 863.
[30] J. Mijovic, N. Miura, T. Monetta, Y. Duan, Polym. News 26 (2001) 251.
[31] J. Mijovic, S. Andjelic, Polymer 36 (1995) 3783.
[32] C.A. Angell, Polymer 38 (1997) 6263.
[33] S. Havriliak, S. Negami, J. Polym. Sci. Part C 14 (1966) 99.
[34] G. Williams, D.C. Watts, Trans. Faraday Soc. 66 (1970) 80.
[35] (a) E.W. Fischer, A. Zetsche, Polym. Preprints (Am. Chem. Soc. Div. Polym. Chem.) 33 (1992) 78;
(b) G. Katana, E.W. Fischer, Th. Hack, V. Abetz, F. Kremer, Macromolecules 28 (1995) 2714;
(c) S. Kamath, R.H. Colby, S. Kumar, K. Karatasos, G. Floudas, G. Fytas, J.E.L. Roovers, J. Chem. Phys. 111 (1999) 6121.
[36] C.M. Roland, K.L. Ngai, Macromolecules 25 (1992) 363.
[37] K.L. Ngai, J. Non-Cryst. Solids 275 (2000) 7.
[38] (a) C.A. Angell, Science 267 (1995) 1924;
(b) R. Richert, C.A. Angell, J. Chem. Phys. 108 (1998) 9016.
[39] J. Fournier, G. Williams, C. Duch, G.A. Aldridge, Macromolecules 29 (1996) 7097.
[40] B. Fitz, J. Mijovic, Macromolecules 32 (1999) 3518.